INTERNATIONAL
ENDODONTIC JOURNAL

doi:10.1111/iej.13241

The extra domain A of fibronectin facilitates osteoclastogenesis in radicular cysts through vascular endothelial growth factor

J. W. Yang[1,2,3,4], J. H. Jiang[5], H. C. Wang[6] & C. Y. Li[7]

[1]Department of Prosthodontics, Peking University School and Hospital of Stomatology; [2]National Engineering Laboratory for Digital and Material Technology of Stomatology; [3]Research Center of Engineering and Technology for Digital Dentistry of Ministry of Health; [4]Beijing Key Laboratory of Digital Stomatology; [5]Department of Orthodontics, Peking University School and Hospital of Stomatology, Beijing; [6]Department of Pathology, School & Hospital of Stomatology, Shanghai Engineering Research Center of Tooth Restoration and Regeneration, Tongji University, Shanghai; and [7]The Central Laboratory, Peking University School and Hospital of Stomatology, Beijing, China

Abstract

Yang JW, Jiang JH, Wang HC, Li CY. The extra domain A of fibronectin facilitates osteoclastogenesis in radicular cysts through vascular endothelial growth factor. *International Endodontic Journal*.

Aim To analyse the effects of the alternatively spliced fibronectin (FN) gene and its isoforms on osteoclastogenesis in radicular cysts.

Methodology Specimens of radicular cysts were collected surgically from 22 patients whose radiolucent periapical areas were measured on digital panoramic radiographs before surgery. The associations between the radiolucent areas and FN isoforms, vascular endothelial growth factor (VEGF) expression or micro-vessel density, as well as the relationships amongst them, were analysed by immunohistochemical staining using the antibodies IST-9, BC-1, P1F11, VEGF and CD34. Fibroblasts isolated from those specimens were used to induce Trap + MNCs, and the effects of induction were assessed by blocking FN containing extra domain A (EDA + FN), COX-2 or VEGF *in vitro*. The effects of EDA exon knockout using CRISPR/Cas system were also assessed. Quantitative PCR was used to analyse relative expression of FN isoforms and osteoclastogenic genes. Data were analysed using linear regression, Spearman's rank correlation analysis, chi-square test and Student's *t*-test; $P < 0.05$ was considered significant.

Results Micro-vessel density and EDA + FN staining were positively associated with the size of radiolucent periapical areas (mm^2; $P < 0.05$), consistent with a positive association between Trap + MNCs and VEGF expression in fibroblasts ($P < 0.05$). Blocking the interaction between EDA + FN and fibroblasts inhibited Trap + MNC formation. In addition, EDA exon knockout decreased VEGF expression and inhibited Trap + MNC formation to the extent of blocking VEGF by bevacizumab, but osteoclastogenic induction was restored by recombinant VEGF. Using retrospective clinicopathological data, VEGF staining was shown to be positively associated with EDA + FN staining, micro-vessel density and the size of radiolucent areas ($P < 0.05$).

Conclusion In fibrous capsules of radicular cysts, the alternatively spliced isoform EDA + FN generated by fibroblasts stimulated VEGF expression via an autocrine effect and then facilitated osteoclastogenesis. Both blockage of VEGF and EDA exon knockout could be used to inhibit bone destruction.

Keywords: extra domain A, fibroblast, osteoclastogenesis, radicular cyst, vascular endothelial growth factor.

Received 24 January 2019; accepted 24 October 2019

Correspondence: Cui-Ying Li, The Central Laboratory, Peking University School and Hospital of Stomatology, 22 South Zhongguancun Avenue Haidian District, Beijing 100081, China (e-mail: licuiying_67@163.com).

Jing-wen Yang and Jiu-hui Jiang contributed equally to this article.

Introduction

According to previous studies, fibroblasts isolated from the fibrous capsule of odontogenic cysts induce more osteoclasts than do normal controls (Wang & Li 2013, Wang *et al.* 2015a,b), possibly attributed to the differentiation of myofibroblasts, which are activated during chronic inflammation (Kouhsoltani *et al.* 2016) or inappropriate wound healing (Lemanska-Perek *et al.* 2016). Chronic inflammation may initiate radicular cysts that can also activate fibroblasts in capsules, generating extracellular matrix (ECM; Jiang *et al.* 2014), cellular factors and metabolic products (de Moraes *et al.* 2011, Tekkesin *et al.* 2011, Bernardi *et al.* 2015), leading to osteoclastogenesis and bone destruction, as illustrated by radiolucent periapical areas.

Fibronectin (FN) is the main component of the ECM, and in most normal adult tissues, isoforms containing domains EDA (EDA + FN), EDB (EDB + FN) and IIICS (CS1-FN) are absent (Liu *et al.* 2015, Lv *et al.* 2017). However, myofibroblasts generate these isoforms via alternative splicing of the FN gene, especially during inflammation, wound healing or tumour formation (Kalluri & Zeisberg 2006), suggesting their involvement in bone destruction (Elmusrati*et al.* 2017). In odontogenic tumours or cysts, the stroma contains these activated fibroblasts as well (Kouhsoltani *et al.* 2016), from which EDA + FN can be generated. For instance, EDA + FN is distributed within the stroma of ameloblastoma (Heikinheimo *et al.* 1991). Radicular cysts are initiated by chronic inflammation, and inflammatory factors within the fibrous capsules tend to stimulate generation of EDB + FN and CS1-FN (Boyle *et al.* 2000, Khan *et al.* 2005, Liu *et al.* 2015). Considering the participation of FN isoforms in tumour aggressiveness (Kamarajan *et al.* 2010, Wang *et al.* 2015a,b), bone destruction resulting from odontogenic cysts may be affected by FN isoforms as well.

The effects of FN isoforms on osteoclastogenesis may contribute to bone destruction due to the inflammatory microenvironment of radicular cysts (Khan *et al.* 2005, Khan *et al.* 2012, Liu *et al.* 2015). Since the three main splice variants, EDA + FN, EDB + FN and CS1-FN, are ligands of integrin receptors and Toll-like receptor 4 (TLR4), interactions between FN isoforms and receptors in pre-osteoclasts may directly affect osteoclastogenesis (Doddapattar *et al.* 2015, Jiang *et al.* 2016), whilst their interaction in other cells could alter the expression of osteoclastogenic genes, such as vascular endothelial growth factor (VEGF) or IL-17 (Liu *et al.* 2015, Lv *et al.* 2017), by which osteoclastogenesis can be indirectly influenced. Therefore, this study explored the effects of FN isoforms on bone destruction in radicular cysts, as well as the underlying mechanism through antibody blocking and gene editing using the type II bacterial clustered, regularly interspaced, palindromic repeats (CRISPR)-associated (Cas) system (Kohan *et al.* 2010, Wang *et al.* 2015a,b).

Materials and methods

The standard for radicular cyst case selection

In the Department of Oral and Maxillofacial Surgery, Peking University School and Hospital of Stomatology in 2018, 22 patients (Table 1) with radicular cysts surrounding the apex of root filled teeth or teeth with necrotic pulps were selected, and the radiolucent periapical lesions removed surgically. All were diagnosed as radicular cysts by the Department of Pathology, Peking University School and Hospital of Stomatology. The periods between acute periapical periodontitis and radiographic examination were no greater than 1 year. The cystic lesions had no symptoms of acute inflammation, such as severe, pulsative or spontaneous pain, and purulence, within at least 4 months before surgical excision, and at the same time, patients had not taken antibiotics or inflammatory medications, as described previously (Zizzi *et al.* 2013). All patients gave written consent to use their specimens for research purposes, as approved by the Peking University School of Stomatology Institutional Review Board (Beijing, China; permit number: PKUSSIRB201838112). The clinical data of patients are list in Table 1.

Immunohistochemical investigation

Formalin-fixed specimens from 22 cases were embedded in paraffin, and 4-μm thick slices were prepared, which were stained with antibodies: IST-9, BC-1, CD34 (Abcam Ltd., Cambridge, MA, USA), P1F11 and VEGF (Santa Cruz, Dallas, TX, USA). Negative controls were stained with phosphate-buffered saline (PBS). Biotinylated secondary antibody (1 : 200) incubated the slices for 1 h, and diaminobenzidine (Zhongshan Golden Bridge Biological Technology COLTD, Beijing, China) visualized immunocomplexes.

The staining of EDA + FN, EDB + FN, CS1-FN and VEGF in the stromal area was investigated with a light

Table 1 The clinical data of patients

Gender	Age (year)	Region of lesion	Radiolucent area (mm^2)
F	77	Mandible	58.56510417
M	65	Mandible	140.0486111
M	29	Maxilla	14.84346065
F	31	Mandible	23.6400463
F	43	Maxilla	33.4552336
M	40	Mandible	54.38454861
M	51	Maxilla	83.08854167
F	42	Mandible	101.1047454
F	30	Mandible	102.3738426
M	38	Maxilla	122.9033565
M	51	Mandible	125.9890046
M	62	Maxilla	152.7520255
M	57	Maxilla	174.2395833
F	57	Mandible	177.4496528
F	25	Mandible	214.0792824
F	40	Maxilla	221.9178241
M	60	Mandible	314.1637731
F	64	Mandible	344.0124421
M	52	Mandible	382.3324901
M	46	Mandible	401.6692708
M	65	Mandible	506.6663773
F	33	Mandible	848.455729

microscope (Olympus BX51, Olympus, Tokyo, Japan), and the ratio of integrated optical density (IOD) to stromal area (IOD μm^{-2}) was quantified with Image-Pro Plus ver. 6.0 software (IPP6.0; Media Cybernetics, Silver Spring, MD, USA; Zhang *et al.* 2014), according to the definition of the area of interest: hue, 0–30; saturation, 0–255; and intensity, 0–255. The median IOD μm^{-2} was used to classify groups as high or low expression. In the fibrous capsule surrounding the epithelial lining of cyst, the range within 500 μm from epithelial lining were investigated, in which the micro-vessels areas (μm^2) surrounded by CD34+ endothelia were measured (Jiang *et al.* 2014), and the mean areas (μm^2) from at least five random high-power fields (hpf: 400× magnification) represented the density of micro-vessels. The cases were divided into two groups, according to the median of the FN isoform, VEGF and micro-vessel density, respectively.

This study aimed to analyse the effects of FN isoforms, VEGF or micro-vessel density within the same background of disease; therefore, only radicular cysts were investigated and noninflammatory controls were omitted.

Measuring panoramic radiographs

Digital panoramic radiographs were taken, using a PM 2002 CC Proline X-ray machine (Planmeca OY, Helsinki, Finland) with Kodak T-MAT G/RA Dental Film (Eastman Kodak, Rochester, NY, USA; Persson *et al.* 2003). Consistent with previous studies (Persson *et al.* 2003, Chuenchompoonut *et al.* 2003), from incisor to the region at the condyle, the magnification factor varied within the range of 1.25–1.30. The observer determined the borders of lesions by tracing the outlines, using IPP6.0 software (Media Cybernetics) to calibrate the radiolucent areas (mm^2), by which the range of bone destruction could be assessed. The cases were demarcated as small and large groups according to the median of the areas of radiolucent lesions.

Cell culture

The fibroblasts were successfully isolated from the surgical specimens of 20 in the 22 cases, and the cells from each cases were routinely cultured for *in vitro* analysis, using α-modified Eagle's medium (α-MEM; GIBCO, Grand Island, NY, USA; Wang & Li 2013, Wang *et al.* 2015a,b). Raw264.7, the osteoclast precursor, was grown in Dulbecco's modified Eagle's medium (DMEM) (GIBCO). About 10% foetal bovine serum (FBS), 2 mmol L^{-1} L-glutamine, 100 U ml^{-1} penicillin and 100 g ml^{-1} streptomycin were contained in medium. Cells were maintained in 5% CO_2 atmosphere and 95% humidity, at 37 °C.

Collecting conditioned medium for osteoclastogenic induction

When fibroblasts had grown to 70%–80% confluence (i.e. cells took up 70%–80% area of a dish) in the 100 mm dishes, serum-free α-MEM replaced the previous medium and maintained cells for 7 days. Then, the supernatants were centrifuged for 10 min, at 550 g; and 50% aliquoted supernatant was mixed with 40% fresh α-MEM (GIBCO) as well as 10% FBS, to make conditioned medium (Wang *et al.* 2015a,b). Only six cases had provided sufficient fibroblasts were used to make the conditioned medium.

In 24-well plates, Raw 264.7 were seeded at 1000 cells $well^{-1}$, and recombinant murine RANKL (R & D; 12 ng μL^{-1}) was added into the conditioned medium for osteoclastogenic induction. Raw 264.7 were maintained for 10 days and stained using a tartrate-resistant acid phosphatase (TRAP) Kit (Sigma, St. Louis, MO, USA; Wang & Li 2013, Wang *et al.* 2015a,b, Chen *et al.* 2016). Cells stained with TRAP (Trap+) and containing at least three nuclei (Trap + MNCs) were the osteoclast-like cells.

Excluding EDA exon and modulating conditioned medium

Using the same protocol as in a previous studies (Wang *et al.* 2015a,b, Lv *et al.* 2017), at 70%–90% confluence, cells were cultured in serum-free medium for 6 h, and plasmids containing sequences of single guide (sg) RNAs that complement the DNA flanking EDA were co-transfected, using Lipofectamine 2000, according to manufacturer's protocol (Life Technologies, Carlsbad, CA, USA). Primer sequences and sgRNAs have been described in previous studies (Wang *et al.* 2015a,b, Lv *et al.* 2017, Table 2). These fibroblasts were the EDA knockout group.

According to a previous study (Kohan *et al.* 2010), IST-9 was added into the conditioned medium to block paracrine effects of EDA + FN on pre-osteoclasts (paracrine blocked group), and the autocrine effects on the fibroblasts themselves were blocked by IST-9 in fibroblast cultures (autocrine & paracrine blocked group). NS398 (Sigma) was added into fibroblast cultures to inhibit synthesis of prostaglandin E2 (PGE2) by cyclooxygenase (COX-2) as in a previous study (Wang *et al.* 2015a,b). Bevacizumab (Genentech Inc., South San Francisco, CA, USA) was used to block VEGF in untreated fibroblasts (Kohen *et al.* 2018) (Bevacizumab group), and the recombinant human VEGF (R&D Systems, Minneapolis, MN, USA) was used to restore VEGF levels in EDA knockout fibroblasts (EDA knockout + rhVEGF group).

RNA extraction, reverse transcription and PCR amplification

TRIzol Reagent (Life Technologies) was used to extract RNA from cells, and cDNA was reverse-transcribed from 2 μg total RNA, using superscript first-strand synthesis kit (Life Technologies). The 20 μL mixture was used to conduct real-time PCR; the programme was set with LightCycler real-time PCR system (Roche Diagnostics Ltd, Shanghai, China): 95 °C for 10 min, 40 cycles of annealing/extension at 60 °C (1 min cycle^{-1}) and then denaturation at 95 °C for 15 s (Wang & Li 2013). FN isoforms were assessed in all 20 cases of fibroblasts, and osteoclastogenic genes were assessed in the six cases that were used for collecting conditioned medium. Human β-actin was used to normalize relative expressions (Wang *et al.* 2015a,b). Primers are listed in Table 3.

Statistical analysis

Linear regression, as well as Spearman's rank correlation analysis, were used to assess the associations between IOD μm^{-2} as well as the areas of lesions; the upper case *R* denoted the correlation coefficient of a linear regression, and the Greek letter ρ denoted that of Spearman's rank correlation analysis. Subsequently, the correlation between the VEGF staining and other clinical–pathological characteristics in the fibrous capsules was analysed using chi-square test. Means ± standard deviation (SD) were used to express the quantitative data, and Student's *t*-test was used to analyse the differences between paired groups. $P < 0.05$ was set as the statistical significance. VEGF staining in the groups of clinicopathological characteristics was evaluated with the chi-square test.

Results

Histological and radiographic investigation of radicular cysts

Microscopically, stratified squamous epithelial lining covered the fibrous capsules in which fibroblasts and micro-vessels were distributed; and in some cases, the

Table 2 Sequences of clustered, regularly interspaced, palindromic repeats sgRNA and confirming primers

Name	sgRNA sequence (5′–3′)	PAM sequences (5′–3′)	DSB site in fibronectin (FN) genome (ref|NC_018913.2|)
sgRNA up-stream-F	GTTACAGACATTGATCGCCCTAA	AGG	216251686
sgRNA up-stream-R	AACTTAGGGCGATCAATGTCTGT		
sgRNA down-stream-F	GTTCTGATTGGAACCCAGTCCAC	AGG	216251434
sgRNA down-stream-R	AACGTGGA CTGGGTTCCAATCAG		

	Primers	Product containing EDA	Product without EDA
Primer-down	atagtgggttaattggact	675bp	400bp
Primer-up	agggtaatcacagggag		

Table 3 The primers used for real-time PCR

Fibronectin isoforms (NM_212482)	Forward primers (5′–3′)	Reverse primers (5′–3′)	Sites of amplification
EDA + FN	AGGACTGGCATTCACTGATGTG	GTCACCCTGTACCTGGAAACTTG	5447–5533
EDB + FN	GGTGGACCCCGCTAAACTC	ACCTTCTCCTGCCGCAACTA	4128–4190
CS1-FN	TTCCCCAACTGGTAACCCTT	TTTAAAGCCTGATTCAGACTCG	6520–7229
Total FN	GTGCCACTTCCCCTTCCTAT	ATCCCACTGATCTCCAATGC	1523–1721
Osteoclastogenesis-related genes	**Forward primers (5′–3′)**	**Reverse primers (5′–3′)**	**Gene ID**
IL-6	AACCTgAACCTTCCAAAgATgg	TCTggCTTgTTCCTCACTACT	NM_000600.4
IL-1α	AgATgCCTgAgATACCCAAAACC	CCAAgCACACCCAgTAgTCT	NM_000575.4
TNF-α	gAggCCAAgCCCTggTATg	CgggCCgATTgATCTCAgC	NM_000594.3
M-CSF	AgACCTCgTgCCAAATTACATT	AggTgTCTCATAgAAAgTTCggA	NM_000757.5
VEGFA	TTATgCggATCAAACCTCACC	gAAgCTCATCTCTCCTATgTgC	NM_001171623.1
IL-17	CCggAATACCAATACCAATCCC	AggTggATCggTTgTAgTAATCT	NM_002190.2
COX-2	CCAgTATAAgTgCgATTgTACCC	TCAAAAATTCCggTgTTgAgCA	NM_000963.3
OPG	CACAAATTgCAgTgTCTTTggTC	TCTgCgTTTACTTTggTgCCA	NM_002546.3
RANKL	AgATCgCTCCTCCATgTACCA	gCCTTgCCTgTATCACAAACTT	NM_003839.3
β-actin	CATgTACggTTgCTATCCAggC	CTCCTTAATgTCAcgCACgAT	NM_001101.3

COX, cyclooxygenase; M-CSF, macrophage colony-stimulating factor; VEGF, vascular endothelial growth factor.

needle-like space left by dissolved cholesterol crystals appeared in the fibrous capsules (Fig. 1), coinciding with histological characteristics of radicular cysts (Garcia *et al.* 2007). In connective tissues, staining of FN isoforms was investigated (Fig. 1a–d), and the ratio of IOD to stromal area (IOD μm^{-2}) was used to reflect the expression of each isoform in the fibrous capsules (Zhang *et al.* 2014). The expression of EDA + FN (IOD $\mu m^{-2} = 61.99 \pm 41.58$) was significantly greater than EDB + FN (0.75 ± 0.56, $P < 0.001$) or CS1-FN (0.31 ± 0.31, $P < 0.001$; Fig. 2b). Only EDA + FN expression was positively associated with the sizes of lesions ($n = 22$, $R = 0.634$, $P = 0.002$; Fig. 2a), consistent with Spearman's rank correlation analysis ($\gamma = 0.653$, $P = 0.002$).

Relative expression of FN isoforms and osteoclastogenic effects

In fibroblasts isolated from fibrous capsules, the relative expression of FN isoforms was assessed. Similar to immunohistochemical staining results, mRNA level of EDA + FN (0.5479 ± 0.9655) was the most expressed isoform and much higher than either EDB + FN (0.0719 ± 0.1290, $P = 0.035$) or CS1-FN (0.0018 ± 0.0054, $P = 0.016$; Fig. 2c).

Pre-osteoclasts were induced to form Trap + MNCs by conditioned medium of fibroblasts. In autocrine and paracrine blocked groups, in which interactions between EDA + FN and fibroblasts, as well as pre-osteoclasts, were blocked by IST-9, Trap + MNCs formation was significantly inhibited (5.5833 ± 0.7862), in contrast with untreated (8.7917 ± 0.9939, $P < 0.001$) and paracrine blocked groups (9.2917 ± 1.7643, $P = 0.002$), in which only the interactions between EDA + FN and pre-osteoclasts were blocked. The latter two groups exhibited nonsignificant differences ($P = 0.5930$), suggesting the effects of EDA + FN on fibroblasts themselves, rather than pre-osteoclasts, were critical to osteoclastogenesis (Fig. 2d,e).

Consistently, when the interaction between EDA + FN and fibroblasts was blocked, relative expression of COX-2, TNF-α, VEGF and the ratio of RANKL/OPG were significantly decreased compared to untreated fibroblasts (Fig. 4f, Table 4).

Knockout of EDA exon from the FN gene and inhibition of osteoclastogenesis

As described in previous studies (Wang *et al.* 2015a,b, Lv *et al.* 2017), EDA exon was knocked out from the genome using the CRISPR/Cas system in order to elucidate its role in osteoclastogenesis. As illustrated by the PCR products, EDA knockout fibroblasts generated both the bands containing (675 bp) and without the EDA exon (415 bp; Fig. 3a). All bands without EDA were confirmed by DNA sequencing (Fig. 3c), suggesting the EDA exon had been excluded in some of the cells. Double strain breaks (DSBs) were repaired by nonhomologous end-joining (NHEJ), leading to significantly

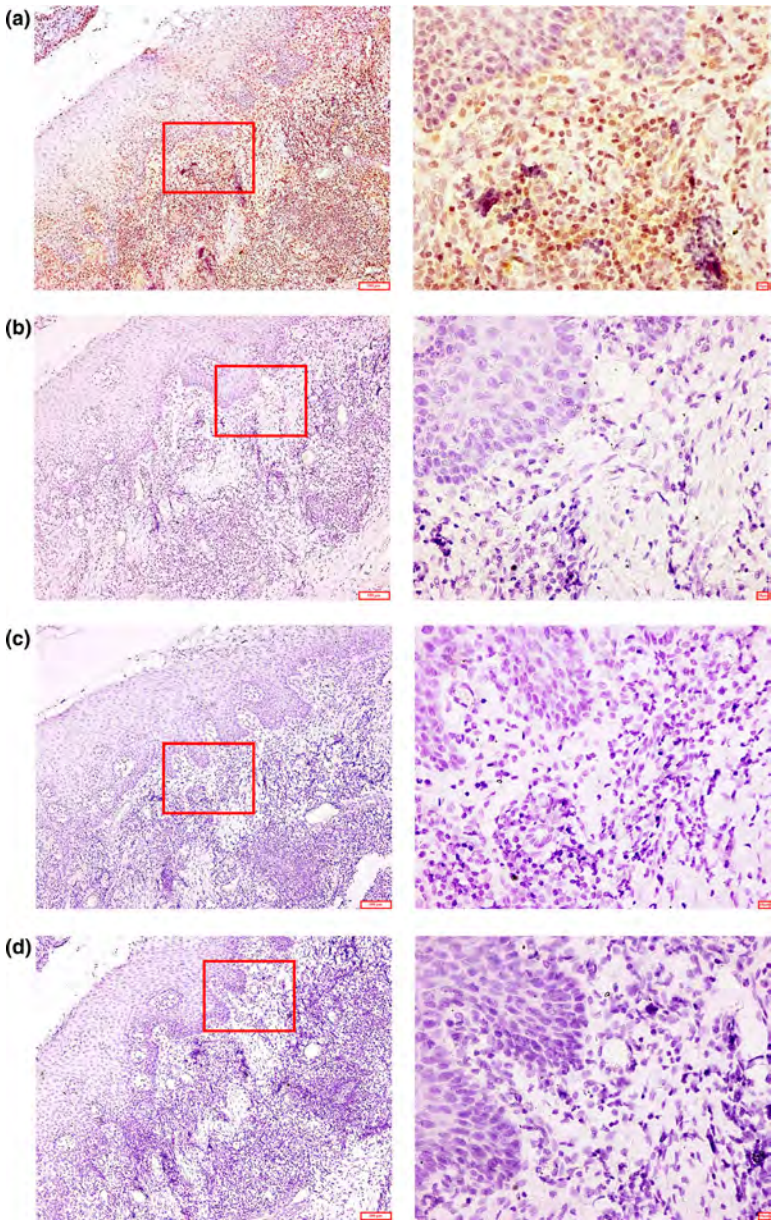

Figure 1 Immunohistochemical staining of fibronectin (FN) isoforms in the stroma of radicular cysts. (a) EDA + FN, (b) EDB + FN, (c) CS1-FN, (d) Negative control (with original magnification ×100, scale bar: 100 μm; local magnification ×400, scale bar: 10 μm).

Figure 2 Relative expression of fibronectin (FN) isoforms and their association with lesion size and Trap + MNCs counting. (a) Positive association between IOD μm^{-2} of EDA + FN in the stroma lesion size (n = 22, R = 0.634, P = 0.002). (b) Immunohistochemical staining (IOD μm^{-2}) comparing FN isoforms within the stroma of radicular cysts. (c) Relative expression of FN isoforms in fibroblasts from fibrous capsules. (d) Comparison of Trap + MNCs counting developed in the untreated, paracrine blocked, as well as autocrine and paracrine blocked groups. (e) Trap + MNCs in the conditioned medium (original magnification ×200, scale bar: 50 μm). (f) Relative expression of osteoclastogenesis-related genes amongst the three groups. $^{*}P < 0.05$; $^{**}P < 0.01$.

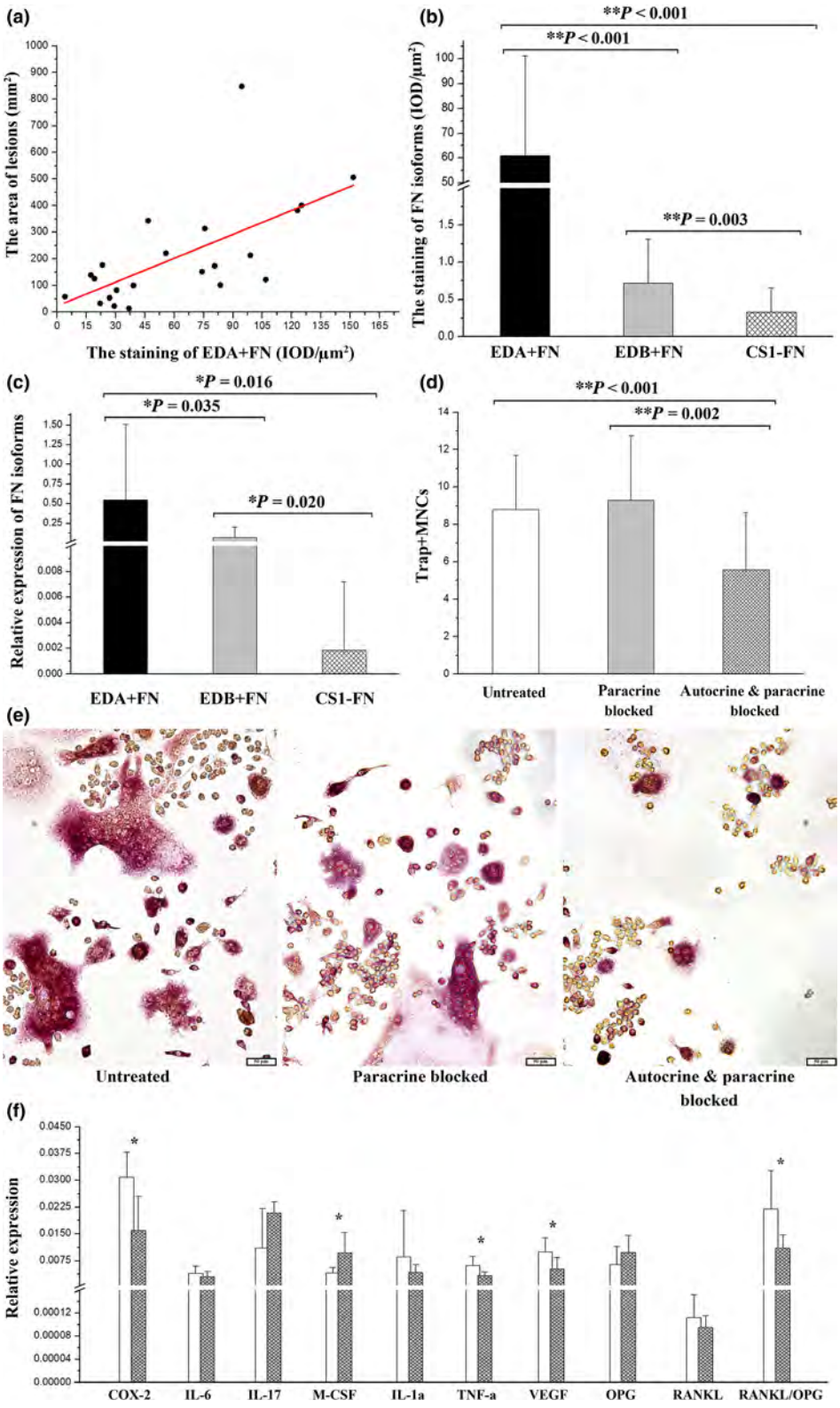

Table 4 Relative expression of genes in the untreated and EDA + FN blocked fibroblasts (Values of relative expression are multiplied by 1000)

Osteoclastogenesis-related genes	Untreated	Antocrine& paracrine blocked	*P*
COX-2	30.9 ± 9.7	16.0 ± 9.5	0.023
IL-6	4.0 ± 2.0	3.1 ± 1.3	0.393
IL-17	11.1 ± 11.0	20.9 ± 3.1	0.063
M-CSF	4.0 ± 1.5	9.6 ± 5.8	0.046*
IL-1α	8.6 ± 13.0	4.2 ± 2.3	0.434
TNF-α	6.1 ± 2.6	3.4 ± 1.0	0.038*
VEGF	9.9 ± 3.9	5.2 ± 3.3	0.046*
OPG	6.5 ± 5.0	9.8 ± 4.8	0.263
RANKL	0.1 ± 0.04	1.0 ± 0.02	0.391
RANKL/OPG	22.0 ± 10.7	11.0 ± 3.7	0.038*

COX, cyclooxygenase; M-CSF, macrophage colony-stimulating factor; VEGF, vascular endothelial growth factor.
*$P < 0.05$.

reduced protein levels of EDA + FN but almost unchanged total FN (Fig. 3b), as in a previous study (Wang *et al.* 2015a,b).

Consequently, conditioned medium from EDA knockout fibroblasts induced significantly less Trap + MNCs than that induced by the untreated group (6.0833 ± 2.6030. vs. 8.7917 ± 0.9939, $P = 0.04$ 381; Fig. 3d,e). However, in EDA knockout fibroblasts, only the relative expression of COX-2 and VEGF was significantly decreased, in contrast with untreated fibroblasts ($P < 0.05$). This is distinct from the IST-9 blocking group mentioned above (Fig. 3f, Table 5).

The effects of COX-2 and VEGF on osteoclastogenesis

Since EDA knockout-induced inhibition of Trap + MNCs seemed to be caused by decreased COX-2 and VEGF, their corresponding inhibitors, NS398 (NS398 group) and bevacizumab (Bevacizumab group), were used to block COX-2 or VEGF, respectively, in fibroblasts of radicular cysts to investigate the effects on osteoclastogenesis. The results revealed that only bevacizumab-treated fibroblasts inhibited Trap + MNC formation (6.1667 ± 2.0535) to a similar level as EDA knockout (6.0833 ± 2.6030, $P = 0.948$) but significantly less than Trap + MNCs developed in the NS398 group (9.1667 ± 1.3844, $P = 0.014$) or in the untreated group (8.7917 ± 0.9939, $P = 0.042$; Fig. 4a,b).

Furthermore, recombinant VEGF (rhVEGF) was added to the conditioned medium from EDA knockout fibroblasts (EDA knockout + rhVEGF group), and rhVEGF restored Trap + MNC formation (9.0416 ± 2.2990) to the approximate extent of untreated group (8.7917 ± 0.9939, $P = 0.839$). Trap + MNCs developed in the EDA knockout + rhVEGF group were also significantly higher than that in the EDA knockout (6.0833 ± 2.6030, $P = 0.047$) or Bevacizumab group (6.1667 ± 2.0535, $P = 0.045$), suggesting EDA-mediated osteoclastogenesisis dependent upon VEGF (Fig. 4a,b).

Retrospective analysis of VEGF expression via clinicopathological data

Clinicopathological data for radicular cysts were analysed again to investigate EDA + FN and CD34 marked micro-vessels. Cases highly expressing VEGF exhibited relatively intense EDA + FN staining ($\chi^2 = 4.545$, $P = 0.033$), as well as a high density of micro-vessels ($\chi^2 = 4.545$, $P = 0.033$; Fig. 5a–c; Table 4). Consistent with the osteoclastogenic effects of VEGF *in vitro*, cases with intensive VEGF staining also exhibited relatively large radiolucent areas ($\chi^2 = 8.909$, $P = 0.003$; Fig. 5d, Table 6). In the radicular cyst, this reiterates the pathway from EDA to VEGF, resulting in bone destruction.

Discussion

Chronic inflammation facilitates alternative splicing of the FN gene (Heikinheimo *et al.* 1991, Boyle *et al.* 2000, Khan *et al.* 2005, Liu *et al.* 2015), generating three FN isoforms, EDA + FN, EDB + FN and CS1-FN.

Figure 3 Exclusion of EDA exon from fibronectin (FN) gene and the consequent osteoclastogenic effects. (a) The bands of PCR products, generated from the genome of EDA knockout and untreated cells. (b) The protein of EDA + FN and total FN, in EDA knockout and untreated cells. (c) Sequencing of the PCR products (415 bp) in which EDA exon was excluded. (d) Trap + MNCs formed in the conditioned medium which was collected from EDA knockout and untreated cells (original magnification ×200, scale bar: 50 μm). (e) The Trap + MNCs counting in the two types of conditioned medium. (f) Relative expression of osteoclastogenesis-related genes amongst the two types of fibroblasts. *$P < 0.05$.

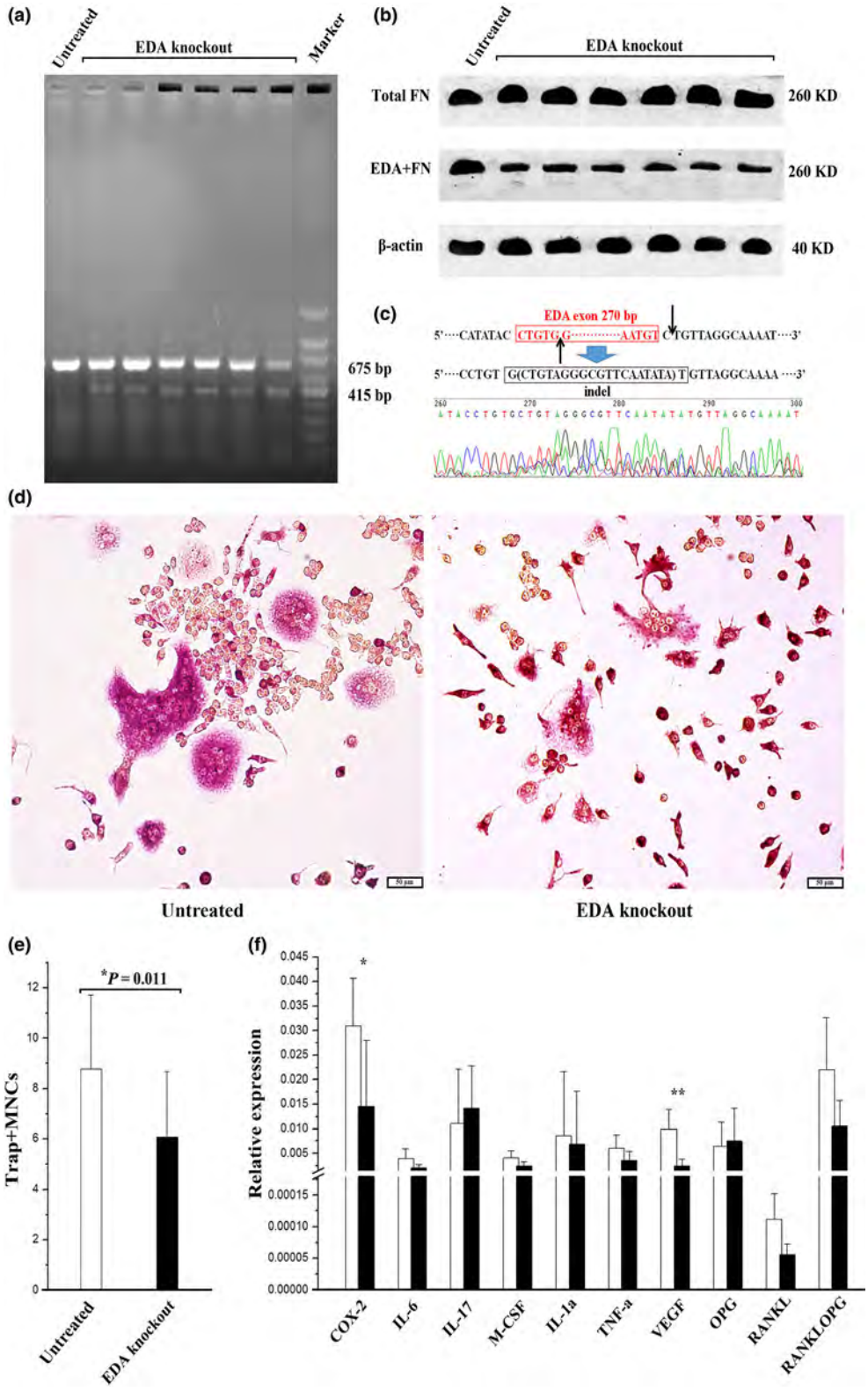

Table 5 Relative expression of genes in the untreated and EDA knockout fibroblasts (Values of relative expression are multiplied by 1000)

Osteoclastogenesis-related genes	Untreated	EDA knockout	*P*
COX-2	30.9 ± 9.7	14.6 ± 13.5	0.037*
IL-6	4.0 ± 2.0	2.1 ± 0.7	0.055
IL-17	11.1 ± 11.0	14.2 ± 8.7	0.596
M-CSF	4.0 ± 1.5	2.5 ± 0.8	0.056
IL-1α	8.6 ± 13.0	6.9 ± 10.8	0.814
TNF-α	6.1 ± 2.6	3.6 ± 1.9	0.082
VEGF	9.9 ± 3.9	2.5 ± 1.3	0.001**
OPG	6.5 ± 5.0	7.5 ± 6.7	0.779
RANKL	0.1 ± 0.04	0.06 ± 0.02	0.052
RANKL/OPG	22.0 ± 10.7	10.6 ± 5.2	0.083

COX, cyclooxygenase; M-CSF, macrophage colony-stimulating factor; VEGF, vascular endothelial growth factor.
*$P < 0.05$; **$P < 0.01$.

In this study, EDA + FN staining was obvious in the fibrous capsule of most radicular cysts and was positively associated with the radiolucent area of lesions, but staining for EDB + FN and CS1-FN was relatively weak. This could be attributed to myofibroblast differentiation, in which EDA + FN plays an essential role (White *et al.* 2008). Myofibroblasts always appear in the fibrous capsule of various odontogenic cysts (Kouhsoltani *et al.* 2016) as the result of chronic inflammation or inappropriate wound healing (Lemanska-Perek *et al.* 2016). Fibroblasts of odontogenic cysts have been demonstrated as favourable for osteoclast formation in previous studies (Wang & Li 2013, Wang *et al.* 2015a,b). This may be partly attributed to the interaction between the EDA fragment and pre-osteoclasts or fibroblasts, hence contributing to osteoclastogenesis either directly or indirectly (Gondokaryono *et al.* 2007, Shinde *et al.* 2008, Xiang *et al.* 2012, Doddapattar *et al.* 2015, Jiang *et al.* 2016).

Consistently, in fibroblasts from the fibrous capsules, the mRNA level of EDA + FN was also much higher than that of EDB + FN and CS1-FN ($P < 0.05$). The specific antibody of EDA + FN, IST-9, blocked the possible interaction between EDA + FN and pre-osteoclasts in conditioned medium (Kohan *et al.* 2010) but did not decrease the counting of Trap + MNCs; however, when IST-9 was added into the fibroblast medium to block the autocrine effects of EDA + FN on fibroblasts themselves, the subsequent conditioned medium induced much fewer Trap + MNCs ($P < 0.05$). This suggests that instead of directly stimulating pre-osteoclasts, EDA + FN contributes to Trap + MNCs formation indirectly. During the interaction between EDA + FN and fibroblasts, expression of osteoclastogenesis-related genes is altered (Khan *et al.* 2005, Gondokaryono *et al.* 2007, Xiang *et al.* 2012, Liu *et al.* 2015). As illustrated in this study, when the autocrine effects of EDA + FN on fibroblasts were blocked by IST-9, the genes facilitating osteoclastogenesis were concomitantly decreased, including COX-2, TNF-α, VEGF and RANKL/OPG (Tekkesin *et al.* 2011, Wang & Li 2013, Wang *et al.* 2015a,b; $P < 0.05$).

In pathological conditions, EDA + FN takes up substantial proportion of total FN (Lv *et al.* 2017); therefore, IST-9 blocks both the EDA + FN and total FN levels. To illustrate the function of the EDA fragment, the EDA exon was knocked out from the genome with the CRISPR/Cas system. Consistent with previous studies (Wang *et al.* 2015a,b, Lv *et al.* 2017) on EDA exon knockout, protein levels of EDA + FN were significantly decreased, but total FN was virtually unchanged. Consequently, conditioned medium from the EDA knockout group developed significantly decreased Trap + MNCs ($P < 0.05$) similar to IST-9 blockage, suggesting that osteoclastogenic induction of EDA + FN could be attributed primarily to function of the EDA fragment, rather than the entire protein. EDA knockout also decreased mRNA levels of COX-2 and VEGF in fibroblasts ($P < 0.05$), but other genes were relatively unchanged. Hence, the EDA fragment may be responsible for the autocrine effects on fibroblasts themselves by which COX-2 or VEGF is secreted to facilitate osteoclastogenesis.

COX-2 facilitates osteoclast formation by synthesizing prostaglandin E2 (PGE2) under pathological conditions (Ogata *et al.* 2007); however, the inhibitor NS398 (Wang *et al.* 2015a,b) could not inhibit Trap + MNCs formation, suggesting little effect of COX-2 on osteoclastogenic induction in this study. In contrast, VEGF antibody, the bevacizumab, significantly inhibited Trap + MNCs formation ($P < 0.05$) as effectively as EDA knockout or IST-9 blockage mentioned above, consistent with the stimulating role of VEGF in osteoclastogenesis (Wang & Li 2013), as it is a substitute for macrophage colony-stimulating factor (M-CSF; Niida *et al.* 1999, Taylor *et al.* 2012). A previous study demonstrated that in odontogenic cysts (Wang & Li 2013), VEGF and COX-2 are involved in the osteoclastogenic

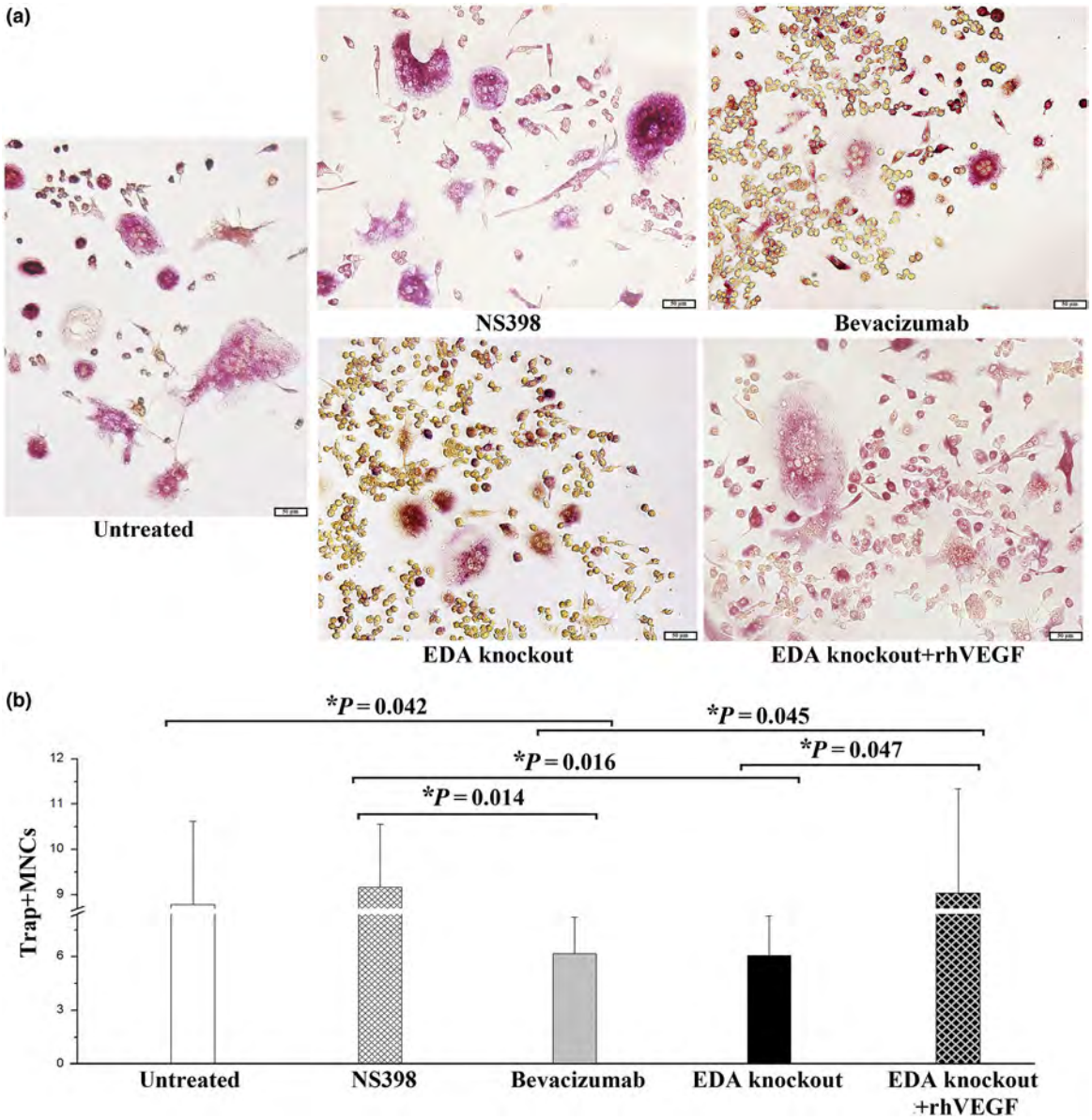

Figure 4 Comparison of Trap + MNCs counting after NS398 inhibited, bevacizumab inhibiting and EDA knockout. (a) Trap + MNCs induced by the five groups of fibroblasts: untreated, NS398 inhibited, bevacizumab inhibited, EDA knockout, and recombinant vascular endothelial growth factor (VEGF) restored fibroblasts (original magnification ×200, scale bar: 50 μm). (b) Trap + MNCs counting induced by the conditioned medium of the five groups. $^*P < 0.05$.

induction of fibroblasts; furthermore, in this study, EDA knockout inhibited Trap + MNC formation, which was restored by addition of exogenous recombinant VEGF (EDA knockout + rhVEGF group) to a level approximate to the untreated group. This suggests that in radicular cysts, the alternatively spliced EDA exon mediates autocrine effects on fibroblasts, resulting in increased VEGF and COX-2, and VEGF is responsible for subsequent osteoclastogenesis.

Retrospective clinicopathological data for radicular cysts revealed that cases highly expressing EDA + FN tend to exhibit intense VEGF staining, along with relatively high vascular density. Pre-osteoclasts can

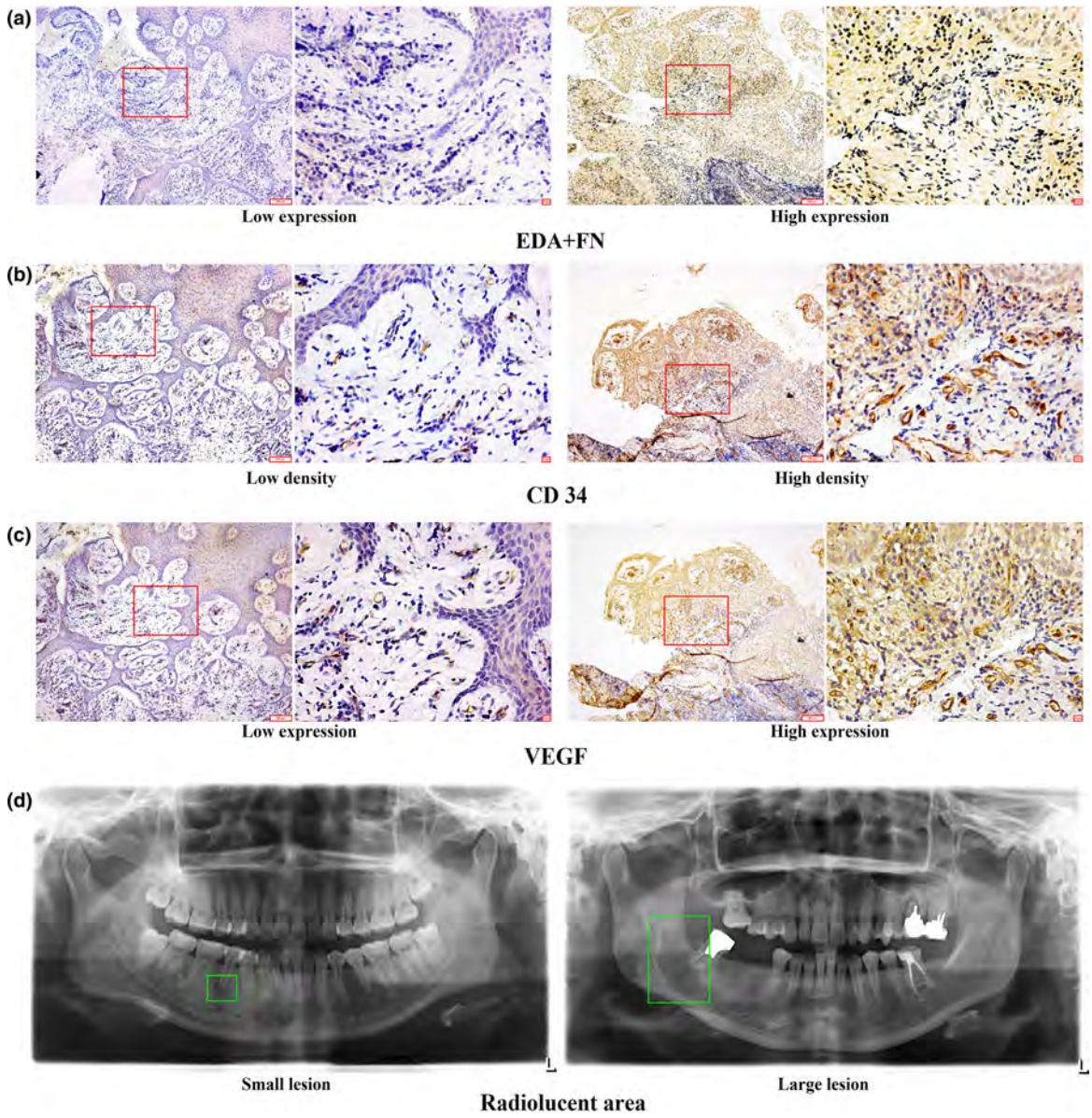

Figure 5 Retrospective analysis of the associations amongst vascularization, FN isoform and lesion size of radicular cysts. (a) Evaluation of EDA + FN staining, within the fibrous capsules of radicular cysts, divided into high and low expression groups. (b) Demarcation of high or low density of micro-vessels according to areas surrounded by CD34 positive endothelia (original magnification ×100; local magnification ×400). (c) Evaluation of vascular endothelial growth factor (VEGF) staining by demarcating high or low expression groups. (original magnification ×100; local magnification ×400). (d) Demarcating the radiolucent areas as large or small areas and evaluating the bone destruction of radicular cysts.

infiltrate from micro-vessels and initiate osteoclastogenesis, together with VEGF itself, leading to obvious bone destruction, as illustrated by radiolucent areas of lesions (Kubota *et al.* 2004). These findings demonstrate a pathway leading from the interaction between EDA and fibroblasts to VEGF-facilitated osteoclastogenesis in radicular cysts. The EDA exon may be a crucial component in changing the microenvironment to favour bone destruction initiated by chronic inflammation.

Table 6 Association between clinical–pathological characteristics and vascular endothelial growth factor (VEGF) staining

Parameters	Low VEGF expression ≤2.2 IOD μm^{-2}	High VEGF expression >2.2 IOD μm^{-2}	χ^2 value	*P*-value
EDA + FN expression				
≤50	8 (72.7%)	3 (27.3%)	4.545	0.033*
>50	3 (27.3%)	8 (72.7%)		
Micro-vessel density				
≤2400 μm^2	8 (72.7%)	3 (27.3%)	4.545	0.033*
>2400 μm^2	3 (27.3%)	8 (72.7%)		
The size of lesion (mm^2)				
≤150	9 (81.8%)	2 (18.2%)	8.909	0.003**
>150	2 (18.2%)	9 (81.8%)		

*$P < 0.05$; **$P < 0.01$.

Conclusions

In fibrous capsules of radicular cysts, the alternatively spliced isoform EDA + FN generated by fibroblasts stimulated VEGF expression via an autocrine effect and then facilitated osteoclastogenesis. Both blockage of VEGF and EDA exon knockout could be used to inhibit bone destruction.

Acknowledgements

This study was financially supported by grants from the National Natural Science Foundation of China (No. 81600836) and a China Postdoctoral Science Foundation (No. 2016M591718), the National Key Research and Development Program of China (2016YFC1102603), and a Peking University School and Hospital of Stomatology grant (PKUSS20180106).

Conflict of interest

The authors have stated explicitly that there are no conflicts of interest in connection with this article.

References

Bernardi L, Visioli F, Nor C, Rados PV (2015) Radicular cyst: an update of the biological factors related to lining epithelium. *Journal of Endodontics* **41**, 1951–61.

Boyle DL, Shi Y, Gay S, Firestein GS (2000) Regulation of CS1 fibronectin expression and function by IL-1 in endothelial cells. *Cellular Immunology* **200**, 1–7.

Chen YW, Wang HC, Gao LH *et al.* (2016) Osteoclastogenesis in local alveolar bone in early decortication-facilitated orthodontic tooth movement. *PLoS ONE* **11**, e0153937.

Chuenchompoonut V, Ida M, Honda E, Kurabayashi T, Sasaki T (2003) Accuracy of panoramic radiography in assessing the dimensions of radiolucent jaw lesions with distinct or indistinct borders. *Dentomaxillofacial Radiology* **32**, 80–6.

Doddapattar P, Gandhi C, Prakash P *et al.* (2015) Fibronectin splicing variants containing extra domain A promote atherosclerosis in mice through toll-like receptor 4. *Arteriosclerosis, Thrombosis and Vascular Biology* **35**, 2391–400.

Elmusrati AA, Pilborough AE, Khurram SA, Lambert DW (2017) Cancer-associated fibroblasts promote bone invasion in oral squamous cell carcinoma. *British Journal of Cancer* **117**, 867–75.

Garcia CC, Sempere FV, Diago MP, Bowen EM (2007) The post-endodontic periapical lesion: histologic and etiopathogenic aspects. *Medicina Oral Patologia Oral Cirrugia Bucal* **12**, E585–90.

Gondokaryono SP, Ushio H, Niyonsaba F *et al.* (2007) The extra domain A of fibronectin stimulates murine mast cells via toll-like receptor 4. *Journal of Leukocyte Biology* **82**, 657–65.

Heikinheimo K, Morgan PR, Happonen RP, Stenman G, Virtanen I (1991) Distribution of extracellular matrix proteins in odontogenic tumours and developing teeth. *Virchows Archiv B Cell Pathology Including Molecular Pathology* **61**, 101–9.

Jiang WP, Sima ZH, Wang HC *et al.* (2014) Identification of the involvement of LOXL4 in generation of keratocystic odontogenic tumors by RNA-Seq analysis. *International Journal of Oral Science* **6**, 31–8.

Jiang H, Si Y, Li Z *et al.* (2016) TREM-2 promotes acquired cholesteatoma-induced bone destruction by modulating TLR4 signaling pathway and osteoclasts activation. *Scientific Reports* **6**, 38761.

Kalluri R, Zeisberg M (2006) Fibroblasts in cancer. *Nature Reviews Cancer* **6**, 392–401.

Kamarajan P, Garcia-Pardo A, D'Silva NJ, Kapila YL (2010) The CS1 segment of fibronectin is involved in human OSCC pathogenesis by mediating OSCC cell spreading, migration, and invasion. *BMC Cancer* **10**, 330.

Khan ZA, Chan BM, Uniyal S *et al.* (2005) EDB fibronectin and angiogenesis – a novel mechanistic pathway. *Angiogenesis* **8**, 183–96.

Khan MM, Gandhi C, Chauhan N *et al.* (2012) Alternatively-spliced extra domain A of fibronectin promotes acute inflammation and brain injury after cerebral ischemia in mice. *Stroke* **43**, 1376–82.

Kohan M, Muro AF, White ES, Berkman N (2010) EDA-containing cellular fibronectin induces fibroblast differentiation through binding to alpha4beta7 integrin receptor and MAPK/Erk 1/2-dependent signaling. *FASEB Journal* **24**, 4503–12.

Kohen MC, Tatlipinar S, Cumbul A, Uslu U (2018) The effects of bevacizumab treatment in a rat model of retinal ischemia and perfusion injury. *Molecular Vision* **24**, 239–50.

Kouhsoltani M, Halimi M, Jabbari G (2016) Immunohistochemical evaluation of myofibroblast density in odontogenic cysts and tumors. *Journal of Dental Research Dental Clinics Dental Prospects* **10**, 37–42.

Kubota Y, Yamashiro T, Oka S, Ninomiya T, Ogata S, Shirasuna K (2004) Relation between size of odontogenic jaw cysts and the pressure of fluid within. *British Journal of Oral & Maxillofacial Surgery* **42**, 391–5.

Lemanska-Perek A, Krzyzanowska-Golab D, Pupek M, Klimeczek P, Witkiewicz W, Katnik-Prastowska I (2016) Analysis of soluble molecular fibronectin-fibrin complexes and EDA-fibronectin concentration in plasma of patients with atherosclerosis. *Inflammation* **39**, 1059–68.

Liu H, Dolkas J, Hoang K *et al.* (2015) The alternatively spliced fibronectin CS1 isoform regulates IL-17A levels and mechanical allodynia after peripheral nerve injury. *Journal of Neuroinflammation* **12**, 158.

Lv WQ, Wang HC, Peng J, Wang YX, Jiang JH, Li CY (2017) Gene editing of the extra domain A positive fibronectin in various tumors, amplified the effects of CRISPR/Cas system on the inhibition of tumor progression. *Oncotarget* **8**, 105020–36.

de Moraes M, de Lucena HF, de Azevedo PR, Queiroz LM, Costa Ade L (2011) Comparative immunohistochemical expression of RANK, RANKL and OPG in radicular and dentigerous cysts. *Archives of Oral Biology* **56**, 1256–63.

Niida S, Kaku M, Amano H *et al.* (1999) Vascular endothelial growth factor can substitute for macrophage colony-stimulating factor in the support of osteoclastic bone resorption. *Journal of Experimental Medicine* **190**, 293–8.

Ogata S, Kubota Y, Yamashiro T *et al.* (2007) Signaling pathways regulating IL-1alpha-induced COX-2 expression. *Journal of Dental Research* **86**, 186–91.

Persson RE, Tzannetou S, Feloutzis AG, Bragger U, Persson GR, Lang NP (2003) Comparison between panoramic and intra-oral radiographs for the assessment of alveolar bone levels in a periodontal maintenance population. *Journal of Clinical Periodontology* **30**, 833–9.

Shinde AV, Bystroff C, Wang C *et al.* (2008) Identification of the peptide sequences within the EIIIA (EDA) segment of fibronectin that mediate integrin alpha9beta1-dependent cellular activities. *Journal of Biological Chemistry* **283**, 2858–70.

Taylor RM, Kashima TG, Knowles HJ, Athanasou NA (2012) VEGF, FLT3 ligand, PlGF and HGF can substitute for M-CSF to induce human osteoclast formation: implications for giant cell tumour pathobiology. *Laboratory Investigation* **92**, 1398–406.

Tekkesin MS, Mutlu S, Olgac V (2011) The role of RANK/RANKL/OPG signalling pathways in osteoclastogenesis in odontogenic keratocysts, radicular cysts, and ameloblastomas. *Head and Neck Pathology* **5**, 248–53.

Wang HC, Li TJ (2013) The growth and osteoclastogenic effects of fibroblasts isolated from keratocystic odontogenic tumor. *Oral Diseases* **19**, 162–8.

Wang HC, Jiang WP, Sima ZH, Li TJ (2015a) Fibroblasts isolated from a keratocystic odontogenic tumor promote osteoclastogenesis in vitro via interaction with epithelial cells. *Oral Diseases* **21**, 170–7.

Wang HC, Yang Y, Xu SY, Peng J, Jiang JH, Li CY (2015b) The CRISPR/Cas system inhibited the pro-oncogenic effects of alternatively spliced fibronectin extra domain A via editing the genome in salivary adenoid cystic carcinoma cells. *Oral Diseases* **21**, 608–18.

White ES, Baralle FE, Muro AF (2008) New insights into form and function of fibronectin splice variants. *Journalof Pathology* **216**, 1–14.

Xiang L, Xie G, Ou J, Wei X, Pan F, Liang H (2012) The extra domain A of fibronectin increases VEGF-C expression in colorectal carcinoma involving the PI3K/AKT signaling pathway. *PLoS ONE* **7**, e35378.

Zhang H, Zhang L, Chen L, Li W, Li F, Chen Q (2014) Stromal cell-derived factor-1 and its receptor CXCR4 are upregulated expression in degenerated intervertebral discs. *International Journal of Medical Sciences* **11**, 240–5.

Zizzi A, Aspriello SD, Ferrante L *et al.* (2013) Immunohistochemical correlation between micro-vessel density and lymphoid infiltrate in radicular cysts. *Oral Disease* **19**, 92–9.

